Inorg. Chem. **1998,** *37,* 270−278

Synthesis, X-ray Structures, and Spectroscopic and Electrochemical Properties of (μ-Oxo)bis(μ-carboxylato)diruthenium Complexes Having Six Imidazole Bases as Terminal Ligands

Chellamma Sudha, Sisir K. Mandal, and Akhil R. Chakravarty*

Department of Inorganic and Physical Chemistry, Indian Institute of Science, Bangalore-560 012, India

Received April 4, 1997

Complexes $[Ru_2O(O_2CR)_2(1\text{-}MeIm)_6](ClO_4)_2$ (**1a−c**), $[Ru_2O(O_2CR)_2(ImH)_6](ClO_4)_2$ (**2a,b**), and $[Ru_2O(O_2CR)_2(4\text{-}MeImH)_6](ClO_4)_2$ (**3a,b**) with a (μ-oxo)bis(μ-carboxylato)diruthenium(III) core have been prepared by reacting $Ru_2Cl(O_2CR)_4$ with the corresponding imidazole base, *viz.* 1-methylimidazole (1-MeIm), imidazole (ImH), and 4-methylimidazole (4-MeImH) in methanol, followed by treatment with $NaClO_4$ in water (R: Me, **a**; C_6H_4-*p*-OMe, **b**; C_6H_4-*p*-Me, **c**). Diruthenium(III,IV) complexes $[Ru_2O(O_2CR)_2(1\text{-}MeIm)_6](ClO_4)_3$ (R: Me, **4a**; C_6H_4-*p*-OMe, **4b**; C_6H_4-*p*-Me, **4c**) have been prepared by one-electron oxidation of **1** in MeCN with $K_2S_2O_8$ in water. Complexes **1a**, **2a**·$3H_2O$, and **4a**·$1.5H_2O$ have been structurally characterized. Crystal data for the complexes are as follows: **1a**, orthorhombic, $P2_12_12_1$, $a = 7.659(3)$ Å, $b = 22.366(3)$ Å, $c = 23.688(2)$ Å, $V = 4058(2)$ Å^3, $Z = 4$, $R = 0.0475$, and $R_w = 0.0467$ for 2669 reflections with $F_o > 2\sigma(F_o)$; **2a**·$3H_2O$, triclinic, $P\bar{1}$, $a = 13.735(3)$ Å, $b = 14.428(4)$ Å, $c = 20.515(8)$ Å, $\alpha = 87.13(3)°$, $\beta = 87.61(3)°$, $\gamma = 63.92(2)°$, $V = 3646(2)$ Å^3, $Z = 4$, $R = 0.0485$ and $R_w = 0.0583$ for 10 594 reflections with $F_o > 6\sigma(F_o)$; **4a**·$1.5H_2O$, triclinic, $P\bar{1}$, $a = 11.969(3)$ Å, $b = 12.090(6)$ Å, $c = 17.421(3)$ Å, $\alpha = 108.93(2)°$, $\beta = 84.42(2)°$, $\gamma = 105.97(2)°$, $V = 2292(1)$ Å^3, $Z = 2$, $R = 0.0567$, and $R_w = 0.0705$ for 6775 reflections with $F_o > 6\sigma(F_o)$. The complexes have a diruthenium unit held by an oxo and two carboxylate ligands, and the imidazole ligands occupy the terminal sites of the core. The Ru−Ru distance and the $Ru-O_{oxo}-Ru$ angle in **1a** and **2a**·$3H_2O$ are 3.266(1), 3.272(1) Å and 122.4(4), 120.5(2)°, while in **4a**·$1.5H_2O$ these values are 3.327(1) Å and 133.6(2)°. The diruthenium(III) complexes **1−3** are blue in color and they exhibit an intense visible band in the range 560−575 nm. The absorption is charge transfer in nature involving the Ru(III)-dπ and O_{oxo}-pπ orbitals. The diruthenium(III,IV) complexes are red in color and show an intense band near 500 nm. The diruthenium(III) core readily gets oxidized with $K_2S_2O_8$ forming quantitatively the diruthenium(III,IV) complex. The visible spectral record of the conversion shows an isosbestic point at 545 nm for **1** and at 535 nm for **2** and **3**. Protonation of the oxide bridge by $HClO_4$ in methanol yields the $[Ru_2(\mu\text{-}OH)(\mu\text{-}O_2CR)_2]^{3+}$ core. The hydroxo species shows a visible band at 550 nm. The pK_a value for **1a** is 2.45. The protonated species are unstable. The 1-MeIm species converts to the diruthenium(III,IV) core, while the imidazole complex converts to $[Ru(ImH)_6]^{3+}$ and some uncharacterized products. Complex $[Ru(ImH)_6](ClO_4)_3$ has been structurally characterized. The diruthenium(III) complexes are essentially diamagnetic and show characteristic ^1H NMR spectra indicating the presence of the dimeric structure in solution. The diruthenium(III,IV) complexes are paramagnetic and display rhombic EPR spectral features. Complexes **1−3** are redox active. Complex **1** shows the one-electron reversible $Ru^{III}_2/Ru^{III}Ru^{IV}$, one-electron quasireversible $Ru^{III}Ru^{IV}/Ru^{IV}_2$, and two-electron quasireversible Ru^{III}_2/Ru^{II}_2 couples near 0.4, 1.5, and −1.0 V *vs* SCE in MeCN−0.1 M TBAP, respectively, in the cyclic and differential pulse voltammetric studies. Complexes **2** and **3** exhibit only reversible $Ru^{III}_2/Ru^{III}Ru^{IV}$ and the quasireversible $Ru^{III}Ru^{IV}/Ru^{IV}_2$ couples near 0.4 and 1.6 V *vs* SCE, respectively. The observation of a quasireversible one-step two-electron transfer reduction process in **1** is significant considering its relevance to the rapid and reversible Fe^{III}_2/Fe^{II}_2 redox process known for the tribridged diiron core in the oxy and deoxy forms of hemerythrin.

Introduction

One important aspect in the chemistry of (μ-oxo)bis(μ-carboxylato)dimetal complexes is the electrochemical behavior of the core. In the active site of deoxyhemerythrin, the dioxygen binding to the vacant site of deoxyHr having a $[Fe_2(\mu\text{-}OH)(\mu\text{-}O_2CR)_2]^+$ core is rapid and reversible involving a single-step two-electron transfer redox process, $[Fe^{II}Fe^{II}] \rightleftharpoons [Fe^{III}Fe^{III}]$, along with a concomitant internal proton transfer from the bridging hydroxo group to the peroxide.[1] The hydroperoxide ligand fills the sixth coordination site of oxyHr. The conversion between $[Fe^{II}-OH-Fe^{II}]^{3+}$ and $[Fe^{III}-O-Fe^{III}]^{4+}$ is reversible. The proton shift facilitates transfer of an electron from the second iron(II) to the dioxygen ligand. A similar redox process is presently unknown among synthetic model diiron and related transition-metal complexes.[2−5]

Several (μ-oxo)bis(μ-carboxylato)diiron model complexes having different types of bridging and terminal ligands are

---

(1) (a) Stenkamp, R. E.; Sieker, L. C.; Jensen, L. H.; McCallum, J. D.; Sanders-Loehr, J. *Proc. Natl. Acad. Sci. U.S.A.* **1985**, *82*, 713. (b) Shiemke, A. K.; Loehr, T. M.; Sanders-Loehr, J. *J. Am. Chem. Soc.* **1986**, *108*, 2437. (c) Que, L., Jr.; Scarrow, R. C. *Metal Clusters in Proteins*; American Chemical Society: Washington, DC, 1988; Chapter 8. (d) Reem, R. C.; McCormick, J. M.; Richardson, D. E.; Devlin, F. J.; Stephens, P. J.; Musselman, R. L.; Solomon, E. I. *J. Am. Chem. Soc.* **1989**, *111*, 4688.

S0020-1669(97)00390-X CCC: \$15.00

subjected for thorough investigation[2] following the discovery[6] of such a core structure in the non-heme metalloprotein hemerythrin (Hr). The redox properties of the low molecular weight model complexes are found to be complicated due to the instability of the core on reduction.[7-9] Addition of an electron to the $[Fe_2(\mu\text{-}O)(\mu\text{-}O_2CR)_2]^{2+}$ core forms a mixed-valence $Fe^{II}Fe^{III}$ species which is susceptible to disproportionation or chemical conversion to a different species. Only recently the first mixed-valence diiron(II,III) complex with a $[Fe_2(\mu\text{-}OH)(\mu\text{-}O_2CR)_2]^{2+}$ core has been isolated and structurally characterized.[10] The observation of a second couple $Fe_2^{II}Fe^{III}/Fe^{II}_2$ is thus rare. This is indeed a general observation for all 3d-metal complexes having a $[M_2(\mu\text{-}O)(\mu\text{-}O_2CR)_2]^{2+}$ core.[5,11] The instability of the $M^{II}M^{III}$ core has similarity with the disproportionation nature of the mixed-valence forms of hemerythrin (Hr).[12]

From a chemical point of view, a reversible one-step two-electron transfer process involving two metal centers is unusual when the metals are strongly coupled through an oxide bridge. The reversibility of the electron-transfer process is expected to be poor when there is a considerable change in the structural parameters of the tribridged core on addition or removal of electrons.[13] In addition, there is a possibility of protonation at the oxide ligand when the metals are reduced. There are only a few examples where an irreversible two-electron transfer $M^{III}_2 \rightarrow M^{II}_2$ process is observed in the $[M_2(\mu\text{-}O)(\mu\text{-}O_2CR)_2]^{2+}$ chemistry. In $[Mn_2O(O_2CMe)_2(tacn)_2]^{2+}$, the cathodic peak for the irreversible Mn^{III}_2/Mn^{II}_2 couple is known to appear at −0.5 V *vs* SCE (tacn, triazacyclononane).[14] The dimeric core of $[Fe_2O(O_2CMe)_2\{HB(pz)_3\}_2]$ is known to undergo a chemical conversion $Fe^{III}_2 \rightarrow 2Fe^{II}$ on electrochemical reduction.[15] Interestingly, complexes containing 4d-metals like molybdenum or ruthenium are known to exhibit extensive redox chemistry involving the tribridged core. Although 4d-metal complexes lack any direct relevance to the diiron active centers in non-heme metalloproteins, they can provide useful information on the redox activity of the tribridged core.[16-27] For example, the diruthenium(III) cores in $[Ru_2O(O_2CMe)_4(PPh_3)_2]$ and $[Ru_2O(O_2CO)_2\{HC(pz)_3\}_2]$ undergo an irreversible two-electron reduction at −0.99 and −0.63 V *vs* SCE, respectively.[20,26] In a preliminary communication, we have reported a novel quasi-reversible one-step two-electron transfer reduction process Ru^{III}_2/Ru^{II}_2 involving the tribridged core in $[Ru_2O(O_2CMe)_2(1\text{-}MeIm)_6](ClO_4)_2$ (1-MeIm = 1-methylimidazole).[27] The work is now extended using other imidazole bases viz., imidazole (ImH) and 4-methylimidazole (4-MeImH) and bridging aryl carboxylates. Herein, we report the full details of the results on complexes of composition $[Ru_2O(O_2CR)_2L_6](ClO_4)_2$ (R = Me (**a**), C_6H_4-*p*-X (X = OMe (**b**), Me (**c**)); L = 1-MeIm (**1**), ImH (**2**), 4-MeImH (**3**)). The one-electron oxidized product of **1** and a monomeric species $[Ru(ImH)_6](ClO_4)_3$ (**5**), obtained from the protonation of **2**, have also been isolated and structurally characterized.

Experimental Section

Materials and Methods. Solvents and reagents used for the preparative procedures were obtained from commercial sources. The starting complexes $Ru_2Cl(O_2CR)_4$ (R = Me, C_6H_4-*p*-X (X = OMe, Me)) were prepared by following literature procedures.[26,28]

Measurements. The elemental analyses were obtained from a Heraeus CHN-O Rapid instrument. Conductivity measurements were

---

(2) Lippard, S. J. *Angew. Chem., Int. Ed. Engl.* **1988**, *27*, 344. Wieghardt, K. *Angew. Chem., Int. Ed. Engl.* **1989**, *28*, 1153. Que, L., Jr. *Prog. Inorg. Chem.* **1990**, *38*, 98. Kurtz, D. M., Jr. *Chem. Rev.* **1990**, *90*, 585. Vincent, J. B.; Olivier-Lilley, G. L.; Averill, B. A. *Chem. Rev.* **1990**, *90*, 1447. Wilkins, R. G. *Chem. Soc. Rev.* **1992**, *21*, 171. Feig, A. L.; Lippard, S. J. *Chem. Rev.* **1994**, *94*, 759. Stenkamp, R. E.; *Chem. Rev.* **1994**, *94*, 715. Que, L., Jr.; Dong, Y. *Acc. Chem. Res.* **1996**, *29*, 190. Kim, K.; Lippard, S. J. *J. Am. Chem. Soc.* **1996**, *118*, 4914. Feig, A. L.; Masschelein, A.; Bakac, A.; Lippard, S. J. *J. Am. Chem. Soc.* **1997**, *119*, 334.

(3) Wieghardt, K. *Angew. Chem., Int. Ed. Engl.* **1989**, *28*, 1153. Wieghardt, K. *Angew. Chem., Int. Ed. Engl.* **1994**, *33*, 725. Tanase, T.; Lippard, S. J. *Inorg. Chem.* **1995**, *34*, 4682. Corbella, M.; Costa, R.; Ribas, J.; Fries, P. H.; Latour, J.-M.; Ohrstrom, L.; Solans, X.; Rodriguez, V. *Inorg. Chem.* **1996**, *35*, 1857. Darovsky, A.; Kezerashvili, V.; Coppens, P.; Weyhermüller, T.; Hummel, H.; Wieghardt, K. *Inorg. Chem.* **1996**, *35*, 6916.

(4) Halerow, M. A.; Christou, G. *Coord. Chem. Rev.* **1994**, *94*, 2421. Volkmer, D.; Horstmann, A.; Griesar, K.; Hasse, W.; Krebs, B. *Inorg. Chem.* **1996**, *35*, 1132.

(5) Wieghardt, K.; Llussar, R. M.; Nuber, B.; Weiss, J. *Inorg. Chem.* **1988**, *27*, 721. Bonder, A.; Druke, S.; Wieghardt, K.; Nuber, B.; Weiss, J. *Angew. Chem., Int. Ed. Engl.* **1990**, *29*, 68. Koppen, M.; Fresen, G; Martin, L. L.; Wieghardt, K.; Blondin, G.; Girerd, J. J.; Nuber, B.; Weiss, J. *J. Chem. Soc., Chem. Commun.* **1990**, 1767. Carrano, C. J.; Verastgue, R.; Bond, M. R. *Inorg. Chem.* **1993**, *32*, 3589.

(6) Stenkamp, R. E.; Sieker, L. C.; Jensen, L. H.; Sanders-Loehr, J. *Nature (London)* **1981**, *291*, 263. Stenkamp, R. E.; Sieker, L. C.; Jensen, L. H. *J. Am. Chem. Soc.* **1984**, *106*, 618.

(7) Hartman, J. R.; Rardin, R. L.; Chaudhuri, P.; Pohl, K.; Wieghardt, K.; Nuber, B.; Weiss, J.; Papaefthymiou, G. C.; Frankel, R. B.; Lippard, S. J. *J. Am. Chem. Soc.* **1987**, *109*, 7387.

(8) Kodera, M.; Shimakoshi, H.; Nishimura, M.; Okawa, H.; Iijima, S.; Kano, K. *Inorg. Chem.* **1996**, *35*, 4967.

(9) Vincent, J. B.; Huffman, J. C.; Christou, G.; Li, Q.; Nanny, M. A.; Hendrickson, D. N.; Fong, R. H.; Fish, R. H. *J. Am. Chem. Soc.* **1988**, *110*, 6898. Feng, X.; Bott, S. G.; Lippard, S. J. *J. Am. Chem. Soc.* **1989**, *111*, 8046.

(10) Bossek, U.; Hummel, H.; Weyhermüller, T.; Bill, E.; Wieghardt, K. *Angew. Chem., Int. Ed. Engl.* **1995**, *34*, 2642.

(11) Sheats, J. E.; Czernuszewicz, R. S.; Dismukes, G. C.; Rheingold, A. L.; Petrouleas, V.; Stubbe, J.; Armstrong, W. H.; Beer, R. H.; Lippard, S. J. *J. Am. Chem. Soc.* **1987**, *109*, 1435. Mahapatra, S.; Lal, T. K.; Mukherjee, R. *Inorg. Chem.* **1994**, *33*, 1579. Mandal, S. K.; Armstrong, W. H. *Inorg. Chim. Acta* **1995**, *229*, 261.

(12) (a) Oxidation of deoxyHr to the $(\text{semi-met})_O$ and reduction of metHr to the $(\text{semi-met})_R$ are known to occur at 0.06 and −0.13 V *vs* SCE, respectively. Armstrong, F. A.; Harrington, P. C.; Wilkins, R. G. *J. Inorg. Biochem.* **1983**, *18*, 83. (b) Wilkins, P. C.; Wilkins, R. G. *Coord. Chem. Rev.* **1987**, *79*, 195.

(13) Nicholson, R. S.; Shain, I. *Anal. Chem.* **1965**, *37*, 178, 1634.

(14) Wieghardt, K.; Bossek, U.; Ventur, D.; Weiss, J. *J. Chem. Soc., Chem. Commun.* **1985**, 347.

(15) Armstrong, W. H.; Spool, A.; Papaefthymiou, G. C.; Frankel, R. B.; Lippard, S. J. *J. Am. Chem. Soc.* **1984**, *106*, 3653.

(16) Neves, A.; Bossek, U.; Wieghardt, K.; Nuber, B.; Weiss, J. *Angew. Chem., Int. Ed. Engl.* **1988**, *27*, 685. Wieghardt, K.; Bossek, U.; Neves, A.; Nuber, B.; Weiss, J. *Inorg. Chem.* **1989**, *28*, 432.

(17) Sasaki, Y.; Suzuki, M.; Nagasawa, A.; Tokiwa, A.; Ebihara, M.; Yamaguchi, T.; Kabuto, C.; Ochi, T.; Ito, T. *Inorg. Chem.* **1991**, *30*, 4903.

(18) Neubold, P.; Wieghardt, K.; Nuber, B.; Weiss, J. *Inorg. Chem.* **1989**, *28*, 459.

(19) Hotzelmann, R.; Wieghardt, K.; Ensling, J.; Romstedt, H.; Gütlich, P.; Bill, E.; Flörke, U.; Haupt, H. J. *J. Am. Chem. Soc.* **1992**, *114*, 9470.

(20) Llobet, A.; Curry, M. E.; Evans, H. T.; Meyer, T. J. *Inorg. Chem.* **1989**, *28*, 3131.

(21) Gupta, N.; Mukherjee, S.; Mahapatra, S.; Ray, M.; Mukherjee, R. *Inorg. Chem.* **1992**, *31*, 139.

(22) Syamala, A.; Chakravarty, A. R. *Inorg. Chem.* **1991**, *30*, 4699. Syamala, A.; Das, B. K.; Chakravarty, A. R. *Polyhedron* **1992**, *11*, 335. Syamala, A.; Chakravarty, A. R. *Polyhedron* **1993**, *12*, 273, 1545. Syamala, A.; Nethaji, M.; Chakravarty, A. R. *Inorg. Chim. Acta* **1995**, *229*, 33.

(23) Sudha, C.; Chakravarty, A. R. *J. Chem. Soc., Dalton Trans.* **1996**, 2125.

(24) Kikuchi, A.; Fukumoto, T.; Umakoshi, K.; Sasaki, Y.; Ichimura, A. *J. Chem. Soc., Chem. Commun.* **1995**, 2125.

(25) Tanase, T.; Yamada, Y.; Tanaka, K.; Miyazu, T.; Kato, M.; Lee, K.; Sugihara, Y.; Mori, W.; Ichimura, A.; Kinoshita, I.; Yamamoto, Y.; Haga, M.; Sasaki, Y.; Yano, S. *Inorg. Chem.* **1996**, *35*, 6230.

(26) Mitchell, R. W.; Spencer, A.; Wilkinson, G. *J. Chem. Soc., Dalton Trans.* **1973**, 846.

(27) Sudha, C.; Mandal, S. K.; Chakravarty, A. R. *Inorg. Chem.* **1993**, *32*, 3801.

(28) Das, B. K.; Chakravarty, A. R. *Polyhedron* **1988**, *7*, 685.

done for 1.0 mM solutions using a Century CC603 digital conductivity meter at 25 °C. Electronic spectra were recorded with a Hitachi U-3400 spectrophotometer. The ^1H NMR spectra were obtained from Bruker WH-270 and ACF-200 MHz spectrometers using tetramethylsilane (TMS) as the internal reference. EPR spectra were recorded on a Varian E-109 X-band spectrometer working at a microwave frequency of 9.05 GHz. Cyclic and differential pulse voltammetric (CV and DPV) measurements were made using a three-electrode set up on a PAR model 174 polarographic analyzer connected to a Houston Instruments Omnigraphic X-Y recorder and PAR model 253 Versastat Potentiostat/Galvanostat with EG&G electrochemical softwares operating on Windows 95. In the three-electrode configuration, a platinum button, a platinum wire, and a saturated calomel electrode (SCE) were used as working, auxiliary, and reference electrodes, respectively. For all electrochemical measurements 0.1 M tetrabutylammonium perchlorate (TBAP) in acetonitrile solvent was used as a supporting electrolyte. The measurements were made at 25 °C, and the data were uncorrected for junction potentials. Ferrocene was used as a standard to verify the potentials observed against the SCE. The Fe^{II}/Fe^{III} couple of ferrocene was observed at 0.43 V (*vs* SCE) under similar experimental conditions in MeCN containing 0.1 M TBAP at 25 °C. Coulometric measurements were made using a PAR system digital coulometer attached to the model M273.

Preparation of $[Ru_2O(O_2CMe)_2(1\text{-}MeIm)_6](ClO_4)_2$ (1a). A 0.2 g (0.42 mmol) amount of $Ru_2Cl(O_2CMe)_4$ was reacted with 0.3 mL of 1-methylimidazole (3.6 mmol) in 20 mL of MeOH at 25 °C for 0.5 h under stirring conditions. The resultant blue solution was concentrated to ~5 mL, and the solid was precipitated using a cold aqueous solution of $NaClO_4$. The solid was dissolved in CH_2Cl_2, the mixture was filtered, and the filtrate was evaporated to dryness to isolate the analytically pure complex **1a**. Yield: ~70%. Anal. Calcd for $C_{28}H_{42}N_{12}O_{13}Cl_2Ru_2$: C, 32.72; H, 4.09; N, 16.36. Found: C, 32.66; H, 3.97; N, 16.53. Λ_M (MeCN) = 300 Ω^{-1} cm^2 mol^{-1}. λ_{max} = 565 nm (ϵ, 7200 M^{-1} cm^{-1}) in MeCN.

Preparation of $[Ru_2O(O_2CC_6H_4\text{-}p\text{-}X)_2(1\text{-}MeIm)_6](ClO_4)_2$ (X = OMe (1b), Me (1c)). Complexes **1b,c** were prepared by a general procedure in which 0.2 g of $Ru_2Cl(O_2CC_6H_4\text{-}p\text{-}X)_4$ (0.24 mmol) was magnetically stirred with 0.19 mL of 1-MeIm (~2.3 mmol) at 25 °C for 6 h. A blue solution thus obtained was filtered, and a solid was precipitated on addition of an ice-cold aqueous solution of $NaClO_4$. The crude product was isolated and dried over P_4O_{10}. The pure blue complex was obtained by column chromatography using a silica gel column (34 cm length, 1.2 cm diameter) in chloroform. The complex was eluted with a 20:1 v/v mixture of $CHCl_3$−MeOH. Yield: ~50%. Complex **1b**: Anal. Calcd for $C_{40}H_{50}N_{12}O_{15}Cl_2Ru_2$: C, 39.64; H, 4.13; N, 13.87. Found: C, 39.50; H, 4.35; N, 13.62. Λ_M (MeCN) = 240 Ω^{-1} cm^2 mol^{-1}. λ_{max} = 569 nm (ϵ, 6090 M^{-1} cm^{-1}) in MeCN. Complex **1c**: Anal. Calcd for $C_{40}H_{50}N_{12}O_{13}Cl_2Ru_2$: C, 40.72; H, 4.24; N, 14.25. Found: C, 41.13; H, 3.90; N, 14.64. Λ_M (MeCN) = 245 Ω^{-1} cm^2 mol^{-1}. λ_{max} = 571 nm (ϵ, 6650 M^{-1} cm^{-1}) in MeCN.

Preparation of $[Ru_2O(O_2CMe)_2(ImH)_6](ClO_4)_2$ (2a). The complex was prepared by reacting 0.2 g of $Ru_2Cl(O_2CMe)_4$ (0.42 mmol) with 0.2 g of imidazole (2.9 mmol) in 20 mL of MeOH under stirring conditions for 3 h. The blue solution was concentrated to ~10 mL, and the solid was precipitated with a cold aqueous solution of $NaClO_4$. Yield: ~30%. Anal. Calcd for $C_{22}H_{30}N_{12}O_{13}Cl_2Ru_2$: C, 28.00; H, 3.18; N,17.82. Found: C, 28.29; H, 3.32; N, 17.91. Λ_M (MeCN) = 250 Ω^{-1} cm^2 mol^{-1}. λ_{max} = 563 nm (ϵ, 7280 M^{-1} cm^{-1}) in MeCN.

Preparation of $[Ru_2O(O_2CC_6H_4\text{-}p\text{-}OMe)_2(ImH)_6](ClO_4)_2$ (2b). A 0.2 g (0.24 mmol) amount of $Ru_2Cl(O_2CC_6H_4\text{-}p\text{-}OMe)_4$ and 0.15 g of imidazole (2.2 mmol) were refluxed in 20 mL of MeOH for 1 h. The blue solution was filtered, and the product was precipitated with a cold aqueous solution of $NaClO_4$. The solid was isolated and dried over P_4O_{10}. Analytically pure complex **2b** was obtained by column chromatography on a basic alumina column (34 cm length and 1.2 cm diameter). The complex was eluted with a 10:1 v/v $CHCl_3$−MeOH mixture. Yield: ~50%. Anal. Calcd for $C_{34}H_{38}N_{12}O_{15}Cl_2Ru_2$: C, 36.20; H, 3.37; N, 14.91. Found: C, 36.51; H, 3.20; N, 14.74. Λ_M (MeCN) = 230 Ω^{-1} cm^2 mol^{-1}. λ_{max} = 565 nm (ϵ, 5800 M^{-1} cm^{-1}) in MeOH.

Preparation of $[Ru_2O(O_2CMe)_2(4\text{-}MeImH)_6](ClO_4)_2$ (3a). The complex was prepared by following the procedure used for **2a**. Anal. Calcd for $C_{28}H_{42}N_{12}O_{13}Cl_2Ru_2$: C, 32.72; H, 4.09; N,16.35. Found: C, 32.80; H, 4.42; N, 16.21. Λ_M (MeCN) = 250 Ω^{-1} cm^2 mol^{-1}. λ_{max} = 564 nm(ϵ, 6700 M^{-1} cm^{-1}) in MeCN.

Preparation of $[Ru_2O(O_2CC_6H_4\text{-}p\text{-}OMe)_2(4\text{-}MeImH)_6](ClO_4)_2$ (3b). A mixture of 0.4 g (0.48 mmol) of $Ru_2Cl(O_2CC_6H_4\text{-}p\text{-}OMe)_4$ and 0.38 g of 4-MeImH (4.6 mmol) in 20 mL of MeOH was refluxed for 3 h. The solution was filtered, and the solid was precipitated with an ice-cold solution of $NaClO_4$. The complex was purified by column chromatography on a basic alumina column (30 cm length × 1.2 cm diameter) in $CHCl_3$. The blue complex in ~30% yield was eluted from the column using a 10:1 v/v mixture of $CHCl_3$−MeOH. Part of the complex decomposed on the column. Anal. Calcd for $C_{40}H_{50}N_{12}O_{15}Cl_2Ru_2$: C, 39.64; H, 4.13; N, 13.87. Found: C, 39.51; H, 4.24; N, 14.14. Λ_M (MeCN) = 180 Ω^{-1} cm^2 mol^{-1}. λ_{max} = 568 nm (ϵ, 6550 M^{-1} cm^{-1}) in MeCN.

Preparation of $[Ru_2O(O_2CR)_2(1\text{-}MeIm)_6](ClO_4)_3$ (R = Me (4a), $C_6H_4\text{-}p\text{-}OMe$ (4b), $C_6H_4\text{-}p\text{-}Me$ (4c)). The complexes were prepared by following a general procedure in which $[Ru_2O(O_2CR)_2(1\text{-}MeIm)_6](ClO_4)_2$ (**1**) (1 mmol) in MeOH was reacted with an aqueous solution of $K_2S_2O_8$ (1 mmol) at 25 °C. The color of the solution changed gradually from blue to deep red. The product was precipitated out on adding an ice-cold aqueous solution of $NaClO_4$. The solid thus obtained was filtered out, washed with cold water, and finally dried over P_4O_{10}. Yield: ~quantitative. Complex **4a**: Anal. Calcd for $C_{28}H_{42}N_{12}O_{17}Cl_3Ru_2$: C, 29.78; H, 3.72; N, 14.91. Found: C, 29.54; H, 3.42; N, 14.74. Λ_M (MeCN) = 400 Ω^{-1} cm^2 mol^{-1}. λ_{max} = 498 nm (ϵ, 10 600 M^{-1} cm^{-1}) in MeCN. EPR data: $g_1 = 2.12$, $g_2 = 1.86$, $g_3 = 1.39$ ($g_{av} = 1.79$) in MeCN glass at 77 K. Complex **4b**: Anal. Calcd for $C_{40}H_{50}N_{12}O_{19}Cl_3Ru_2$: C, 36.63; H, 3.82; N, 12.82. Found: C, 36.33; H, 4.14; N, 12.45. Λ_M (MeCN) = 370 Ω^{-1} cm^2 mol^{-1}. λ_{max} = 503 nm (ϵ, 7000 M^{-1} cm^{-1}) in MeCN. EPR data: $g_1 = 2.14$, $g_2 = 1.90$, $g_3 = 1.42$ ($g_{av} = 1.82$) in MeCN glass at 77 K. Complex **4c**: Anal. Calcd for $C_{40}H_{50}N_{12}O_{17}Cl_3Ru_2$: C, 37.53; H, 3.91; N, 13.14. Found: C, 37.50; H, 4.15; N, 13.61. Λ_M (MeCN) = 360 Ω^{-1} cm^2 mol^{-1}. λ_{max} = 504 nm (ϵ, 6800 M^{-1} cm^{-1}) in MeCN. EPR data: $g_1 = 2.12$, $g_2 = 1.86$, $g_3 = 1.39$ ($g_{av} = 1.79$) in MeCN glass at 77 K.

Safety Note. *Perchlorate salts of metal complexes with organic ligands are potentially explosive! Only small quantity of material should be prepared, and these should be handled with great caution.*

Solubility and Stability. Complex **1** is soluble in common organic solvents other than benzene and alkanes. Complex **2** shows appreciable solubility only in polar solvents like MeCN, MeOH, H_2O, and DMF. Complex **3** is soluble in polar solvents but not in organic solvents like $CHCl_3$ and CH_2Cl_2. Complex **4** is soluble in common organic solvents other than benzene and alkanes. The complexes are generally stable in the solid as well as in the solution phase except **3b** which shows moderate stablility in the solution phase.

X-ray Crystallographic Procedures for $[Ru_2O(O_2CMe)_2(1\text{-}MeIm)_6](ClO_4)_2$ (1a), $[Ru_2O(O_2CMe)_2(ImH)_6](ClO_4)_2\cdot 3H_2O$ (2a.3H$_2$O), $[Ru_2O(O_2CMe)_2(1\text{-}MeIm)_6](ClO_4)_3\cdot 1.5H_2O$ (4a·1.5H$_2$O), and $[Ru(ImH)_6](ClO_4)_3$ (5). Dark blue crystals of **1a** were obtained by a diffusion technique using a dichloromethane solution of **1a** and petroleum ether. A rectangular shaped crystal of approximate dimensions 0.40 × 0.12 × 0.04 mm was mounted on a glass fiber with epoxy cement. Crystals of **2a**·3H$_2$O were obtained on cooling a solution of the complex in a MeCN−Et$_2$O mixture at 0 °C. The dark blue crystals showed a dark brown color against transmitted light, but the crystals gave a blue solution when dissolved in MeCN. A diamond shaped crystal of approximate size 0.6 × 0.5 × 0.1 mm was mounted on a glass fiber with epoxy cement. Dark red crystals of **4a**·1.5H$_2$O were obtained on slow evaporation of an aqueous solution of the complex at 25 °C. A rectangular shaped crystal of approximate size 0.6 × 0.5 × 0.2 mm was mounted on a glass fiber with epoxy cement.

The crystal orientation matrix and the unit cell parameters were derived from a least-squares fit to the goniometer settings of accurately located 25 reflections in the 2θ range between 16 and 32°. Data were collected on an Enraf-Nonius CAD4 diffractometer fitted with a graphite monochromated Mo Kα radiation. The intensity data collected in the θ limits $4 \leq 2\theta \leq 45°$ (hkl) for **1a**, $4 \leq 2\theta \leq 50°$ ($h \pm k \pm l$) for **2a**·3H$_2$O,

Table 1. Crystallographic Data for $[Ru_2O(O_2CMe)_2(1\text{-}MeIm)_6](ClO_4)_2$ (**1a**), $[Ru_2O(O_2CMe)_2(ImH)_6](ClO_4)_2\cdot3H_2O$ (**2a**$\cdot3H_2O$), $[Ru_2O(O_2CMe)_2(1\text{-}MeIm)_6](ClO_4)_3\cdot1.5H_2O$ (**4a**$\cdot1.5H_2O$), and $[Ru(HIm)_6](ClO_4)_3$ (**5**)

	1a	**2a**$\cdot3H_2O$	**4a**$\cdot1.5H_2O$	**5**
chem formula	$C_{28}H_{42}N_{12}O_{13}Cl_2Ru_2$	$C_{22}H_{36}N_{12}O_{16}Cl_2Ru_2$	$C_{28}H_{45}N_{12}O_{18.5}Cl_3Ru_2$	$C_{18}H_{24}N_{12}O_{12}Cl_3Ru$
fw	1027	997	1154.23	807.9
space group	$P2_12_12_1$ (No. 19)	$P\bar{1}$ (No. 2)	$P\bar{1}$ (No. 2)	$R\bar{3}c$ (No. 167)
a, Å	7.659(3)	13.735(3)	11.969(3)	18.410(1)
b, Å	22.366(3)	14.428(4)	12.090(6)	18.410(1)
c, Å	23.688(2)	20.515(8)	17.421(3)	15.260(1)
α, deg	90.0	87.13(3)	108.93(2)	90.0
β, deg	90.0	87.61(3)	84.42(2)	90.0
γ, deg	90.0	63.92(2)	105.97(2)	90.0
V, Å^3	4058(2)	3646(2)	2292(1)	4479(1)
$\rho_{calcd.}$, g cm^{-3}	1.68	1.77	1.67	1.80
Z	4	4	2	6
T, K	290	290	290	290
λ(Mo Kα), Å	0.7107	0.7107	0.7107	0.7107
μ(Mo Kα), cm^{-1}	9.34	10.37	9.01	8.61
R (F_o)[a]	0.0475	0.0485	0.0567	0.0650
R_w (F_o)[b]	0.0467	0.0583	0.0705	0.0650
g	0.001 265	0.003 302	0.006 185	0.0

[a] $R(F_o) = (\sum||F_o| - |F_c||)/(\sum|F_o|)$. [b] $R_w(F_o) = [(\sum w^{1/2}||F_o| - |F_c||)/(\sum w^{1/2}|F_o|)]$; $w = 1/[\sigma^2(F_o) + gF_o^2]$.

and $4 \le 2\theta \le 50°$ ($h\pm k\pm l$) for **4a**$\cdot1.5H_2O$ were corrected for Lorentz, polarization, and absorption effects.[29] The structures were solved by direct methods using SHELXS-86 and refined by combination of Fourier-synthesis and full-matrix least-squares methods using SHELX-76.[30] The intensity data for **1a** were found to be weak at higher θ angles. The low data to parameter ratio has constrained us to use data with $F_o > 2\sigma(F_o)$ for structure solution and refinement. All calculations were carried out on a VAX88 computer at the computer center of the Indian Institute of Science. Atomic scattering factors were taken from ref 31. Crystallographic data for the complexes are given in Table 1.

All non-hydrogen atoms in **1a** were refined anisotropically. Some of the hydrogen atoms of the complex cation were located from the difference Fourier map, and the rest were put in their calculated positions ($d_{C-H} = 1.08$ Å). The hydrogen atoms were used for structure factor calculations with an isotropic thermal parameter of 0.1 Å^2. The final difference Fourier map was featureless showing the highest peak of 0.33 e/Å^3, located near Ru(1). The crystal structure of the imidazole complex showed the presence of two independent molecules in the asymmetric unit. Other than the complex cations and anions, three additional peaks were located in the difference Fourier map. They were refined as water molecules. The source of water was the solvents used for crystallization. The oxygen atoms of one perchlorate anion of the molecule B were found to be positionally disordered and the site occupancy factor (sof) values for these atoms were refined and the best sof fixed during least-squares refinement. Most of the hydrogen atoms were located from the difference Fourier map, and the remaining were put in their calculated positions constrained to ride on atoms to which they were attached. The hydrogen atoms were used only for F_o/F_c calculations with an isotropic thermal parameter of 0.1 Å^2. All non-hydrogen atoms except the positionally disordered ones of the perchlorate anion were refined anisotropically. In the crystal structure of the diruthenium(III,IV) complex, there were positional disorder problem. The methyl carbon atom C(20) of one of the 1-MeIm ligand was found to be orientationally disordered. The atoms C(20) and C(20′) were refined each with a sof of 0.5. Besides these, three oxygen atoms of one perchlorate anion were found to be positionally disordered. Six peaks were located in the difference Fourier map, and each peak was refined with a sof of 0.5. All non-hydrogen atoms except the disordered ones were refined anisotropically. Some of the hydrogen atoms could be located from the difference Fourier map, and the rest were put in their calculated positions ($d_{C-H} = 1.08$ Å). The significant residual peaks in the difference Fourier map were best modeled for 1.5 H_2O. Perspective views of the cationic complexes in these structures were obtained by the ORTEP program.[32]

The monomeric $[Ru(ImH)_6](ClO_4)_3$ (**5**), prepared by the addition of perchloric acid to a solution of **2a** in MeOH, was isolated as reddish-brown needles by a diffusion technique using the methanol solution of the complex and diethyl ether. There were 657 unique data, of which 513 observed with $F_o > 5\sigma(F_o)$ were used for structure determination using 71 parameters. Selected crystallographic data are given in Table1.

Results and Discussion

Synthesis and Mechanistic Aspects. The complexes **1**−**3** are prepared in high yield by a general procedure in which the polymeric $Ru_2Cl(O_2CR)_4$, having a "paddle-wheel" structure, undergoes facile core conversion on reaction with imidazole bases in methanol (eq 1). This reaction involves a conversion of the $[Ru_2(\mu\text{-}O_2CR)_4]^+$ unit to a $[Ru_2(\mu\text{-}O)(\mu\text{-}O_2CR)_2]^{2+}$ core having six terminal imidazole ligands. The core conversion involves a one-electron oxidation of the diruthenium(II,III) precursor, a cleavage of the Ru−Ru bond of order 2.5, the formation of an oxo bridge, and substitution of two bridging carboxylates and the axial chloride by six terminal imidazole ligands. Complex **4** has been isolated on oxidation of **1** by $K_2S_2O_8$ in water.

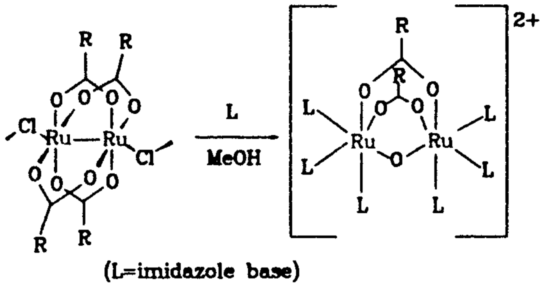

(1)

The formation of the $[Ru_2O(O_2CR)_2]^{2+}$ core from a reaction of $Ru_2Cl(O_2CR)_4$ with PPh_3 in MeOH or MeCN has earlier been reported from our laboratory.[33,34] It has been observed that the

---

(29) North, A. C. T.; Phillips, D. C.; Mathews, F. S. *Acta Crystallogr.* **1968**, *A24*, 351.

(30) Sheldrick, G. M. SHELXS-86, A computer program for Crystal Structure Solution, Universität Göttingen, 1986. SHELX-76, A Program for Crystal Structure Determination, University of Cambridge, 1976.

(31) *International Tables for X-Ray Crystallography*; Kynoch Press: Birmingham, U.K., 1976; Vol. 4.

(32) Johnson, C. K. *ORTEP-II*; Oak Ridge National Laboratory: Oak Ridge, TN, 1976.

(33) Das, B. K.; Chakravarty, A. R. *Inorg. Chem.* **1990**, *29*, 2078.

(34) Das, B. K.; Chakravarty, A. R. *Inorg. Chem.* **1991**, *30*, 4978.

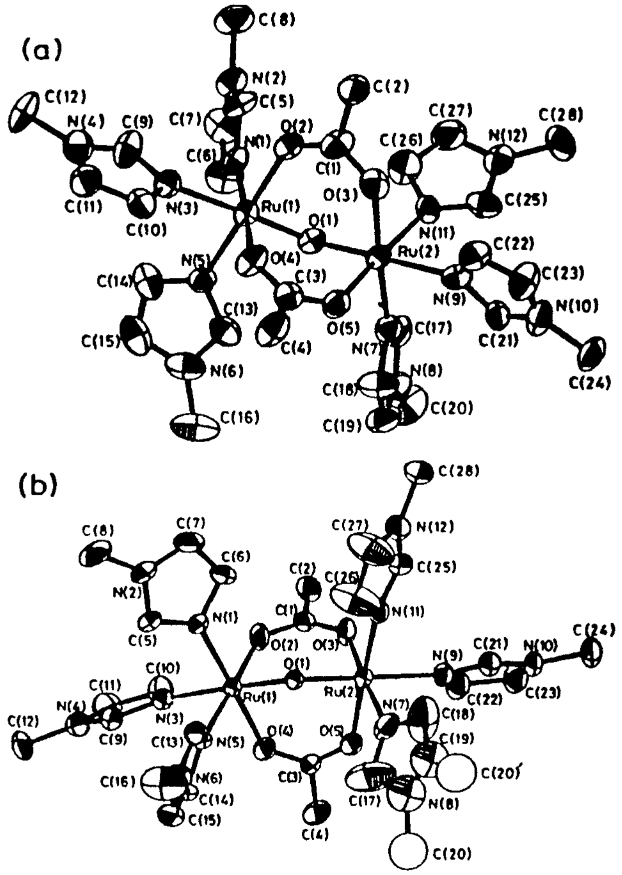

Figure 1. ORTEP view of the complex cations in $[Ru_2O(O_2CMe)_2(1\text{-}MeIm)_6](ClO_4)_2$ (**1a**) (A) and $[Ru_2O(O_2CMe)_2(1\text{-}MeIm)_6](ClO_4)_3{\cdot}1.5H_2O$ (**4a**$\cdot 1.5H_2O$) (B), showing atom-numbering schemes.

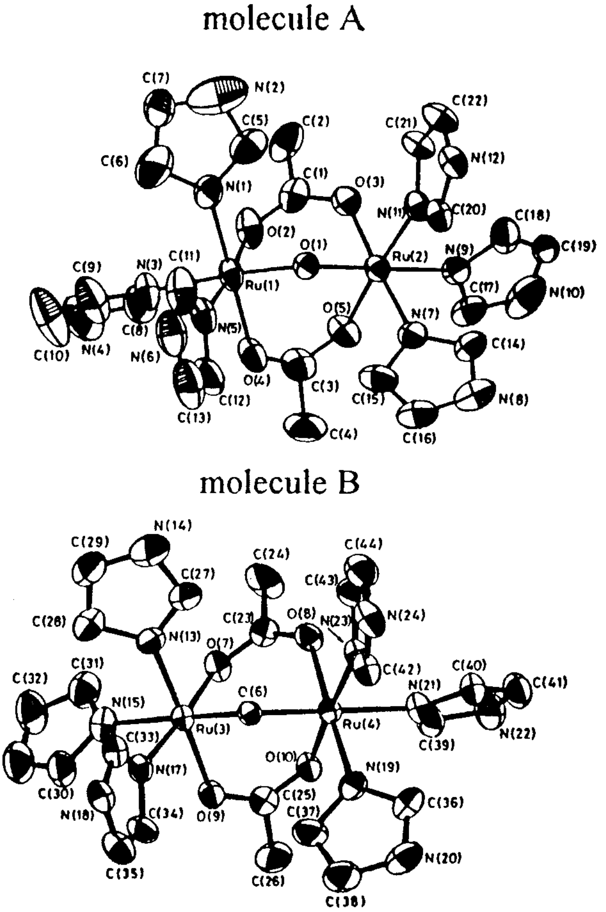

Figure 2. ORTEP diagrams of two independent cationic complexes in $[Ru_2O(O_2CMe)_2(ImH)_6](ClO_4)_2{\cdot}3H_2O$ (molecule A and molecule B).

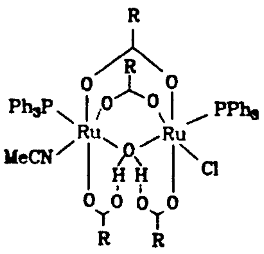

I

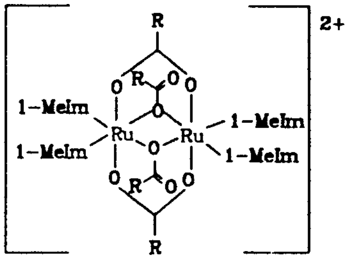

II

initial step of the reaction is the formation of an aquo-bridged class-II type mixed-valence diruthenium(II,III) complex in which the aqua ligand is also involved in an intramolecular hydrogen bonding interaction with two unidentate carboxylate ligands. The (μ-aquo)diruthenium(II,III) core is unstable and undergoes a one-electron oxidation to a (μ-oxo)diruthenium(III) species along with the substitution of two RCO_2H by other terminal ligands. In the present study we are unable to observe the formation of any aquo-bridged species. However, the reaction is believed to proceed through the formation of an ESBO complex as such a species $[Ru_2(O_2CR)_4(1\text{-}MeIm)_4](ClO_4)_2$ has earlier been isolated from a reaction of $Ru_2Cl(O_2CR)_4$ with 1-MeIm.[35] The ESBO complex, which has two three-atom and two monoatomic bridging carboxylate ligands, on further reaction with 1-MeIm forms complex **1**. It appears that the reactions of $Ru_2Cl(O_2CR)_4$ with PPh_3 and the imidazole bases follow different mechanistic pathways involving respective (μ-aquo)diruthenium(II,III) (**I**) and the ESBO diruthenium(III) (**II**) species as the possible intermediates.

Molecular Structures. The complexes $[Ru_2O(O_2CMe)_2(1\text{-}MeIm)_6](ClO_4)_2$ (**1a**), $[Ru_2O(O_2CMe)_2(ImH)_6](ClO_4)_2{\cdot}3H_2O$ (**2a**$\cdot 3H_2O$), and $[Ru_2O(O_2CMe)_2(1\text{-}MeIm)_6](ClO_4)_3{\cdot}1.5H_2O$ (**4a**$\cdot 1.5H_2O$) have been characterized by single-crystal X-ray crystallographic methods. The ORTEP diagrams of the cationic complexes are shown in Figures 1 and 2. Important bond distances and angles are given in Tables 2 and 3. The cationic complexes have a diruthenium unit held by an oxo and two carboxylato ligands. The metal atoms show an essentially octahedral geometry with three bridging atoms occupying a face of the octahedron while the other face is occupied by three terminal unidentate imidazole bases. The complex **2a**$\cdot 3H_2O$ crystallizes with two molecules in the asymmetric unit. The crystal structure of the imidazole complex shows the presence of chemically significant intermolecular hydrogen-bonding interactions involving the nitrogen atom of the imidazole ring and the solvent water molecules [N(6)$\cdots$O(1W), 2.91(1) Å; N(8)$\cdots$O(3W), 2.96(1) Å].

The Ru–Ru distance of 3.27 Å in the $[Ru_2(\mu\text{-}O)(\mu\text{-}O_2CR)_2]^{2+}$ core is considerably shorter than the same observed in the $[Ru_2(\mu\text{-}O)(\mu\text{-}O_2CR)_2]^{3+}$ core. An increase of 0.06 Å in the Ru–Ru distance on one-electron oxidation of the core has resulted from the shortening of the $Ru{-}O_{oxo}$ bond length and an increase in the Ru–O–Ru angle. In the diruthenium(III) complexes the Ru–N bond distances trans to the oxide ligand are considerably longer than the cis Ru–N distances due to the trans effect of the oxide ligand. However, in the diruthenium(III,IV) complex, the trans effect is less prominent. This is an interesting observation as the shorter $Ru{-}O_{oxo}$ bond in the $[Ru_2O]^{5+}$ core

---

[35] Sudha, C.; Mandal, S. K.; Chakravarty, A. R. *Inorg. Chem.* **1994**, *33*, 4878.

Table 2. Selected Bond Distances (Å) and Angles (deg) for $[Ru_2O(O_2CMe)_2(1\text{-}MeIm)_6](ClO_4)_2$ (**1a**) and $[Ru_2O(O_2CMe)_2(1\text{-}MeIm)_6](ClO_4)_3\cdot1.5H_2O$ (**4a**$\cdot1.5H_2O$)

	1a	**4a**$\cdot1.5H_2O$		**1a**	**4a**$\cdot1.5H_2O$
Ru(1)⋯Ru(2)	3.266(1)	3.327(1)	Ru(2)−O(1)	1.867(7)	1.817(3)
Ru(1)−O(1)	1.859(7)	1.803(4)	Ru(2)−O(3)	2.094(7)	2.037(4)
Ru(1)−O(2)	2.057(7)	2.052(3)	Ru(2)−O(5)	2.055(7)	2.061(4)
Ru(1)−O(4)	2.069(7)	2.046(4)	Ru(2)−N(7)	2.054(10)	2.052(7)
Ru(1)−N(1)	2.056(9)	2.036(5)	Ru(2)−N(9)	2.125(9)	2.078(4)
Ru(1)−N(3)	2.157(9)	2.093(5)	Ru(2)−N(11)	2.079(10)	2.028(5)
Ru(1)−N(5)	2.081(9)	2.046(5)			

	1a	**4a**$\cdot1.5H_2O$		**1a**	**4a**$\cdot1.5H_2O$
Ru(1)−O(1)−Ru(2)	122.4(4)	133.6(2)	N(9)−Ru(2)−N(11)	89.7(4)	90.7(2)
N(3)−Ru(1)−N(5)	89.5(4)	90.3(2)	N(7)−Ru(2)−N(11)	91.4(4)	92.4(2)
N(1)−Ru(1)−N(5)	93.8(4)	92.2(2)	N(7)−Ru(2)−N(9)	90.3(4)	91.3(2)
N(1)−Ru(1)−N(3)	90.2(4)	92.3(2)	O(5)−Ru(2)−N(11)	175.2(3)	177.5(2)
O(4)−Ru(1)−N(5)	88.4(3)	89.5(2)	O(5)−Ru(2)−N(9)	85.6(3)	87.2(2)
O(4)−Ru(1)−N(3)	84.5(3)	85.2(2)	O(5)−Ru(2)−N(7)	89.7(3)	89.1(2)
O(4)−Ru(1)−N(1)	174.2(3)	177.0(2)	O(3)−Ru(2)−N(11)	88.2(3)	90.0(2)
O(2)−Ru(1)−N(5)	179.0(3)	176.0(2)	O(3)−Ru(2)−N(9)	86.5(3)	83.7(2)
O(2)−Ru(1)−N(3)	89.9(3)	86.1(2)	O(3)−Ru(2)−N(7)	176.7(3)	174.5(2)
O(2)−Ru(1)−N(1)	87.0(3)	89.6(2)	O(3)−Ru(2)−O(5)	90.5(3)	88.4(2)
O(2)−Ru(1)−O(4)	90.7(3)	88.5(2)	O(1)−Ru(2)−N(11)	89.7(3)	91.6(2)
O(1)−Ru(1)−N(5)	87.2(3)	92.0(2)	O(1)−Ru(2)−N(9)	177.9(3)	175.2(2)
O(1)−Ru(1)−N(3)	176.6(3)	174.9(2)	O(1)−Ru(2)−N(7)	87.7(3)	92.9(2)
O(1)−Ru(1)−N(1)	89.2(3)	92.2(2)	O(1)−Ru(2)−O(5)	95.0(3)	90.4(2)
O(1)−Ru(1)−O(4)	96.2(3)	90.2(2)	O(1)−Ru(2)−O(3)	95.6(3)	92.0(2)
O(1)−Ru(1)−O(2)	93.4(3)	91.5(2)			

is expected to exert greater trans effect than the corresponding $Ru^{III}-O_{oxo}$ bond.

Spectral Properties. The diruthenium(III) complexes **1**−**3** are blue in color, and they exhibit an intense visible band in the range 560−575 nm. The origin of the absorption is believed to be charge transfer in nature involving Ru(III)-dπ and O_{oxo}-pπ orbitals.[20] Diruthenium(III,IV) complexes are red in color and display an intense visible band near 500 nm. The one-electron oxidation of **1**−**3** with potassium persulfate has been monitored using visible spectroscopy. The oxidized product of **1** has been isolated and structurally characterized. The spectral change associated with the conversion of **1a** to **4a** is shown in Figure 3a. The conversion is quantitative, and an isosbestic point is observed at 545 nm. A similar shift has been observed for the complexes **2** and **3** giving an isosbestic point at 535 nm. The diruthenium(III,IV) complexes are paramagnetic and exhibit rhombic EPR spectral patterns.

Protonation of the oxide bridge in the diruthenium(III) complexes with $HClO_4$ in methanol yields the corresponding hydroxo species showing a visible band near 500 nm. The hydroxo species on addition of triethylamine converts to the oxo complex. Figure 3b displays the visible spectral record of the protonation of **1a**. The λ_{max} shifts from 565 nm to 500 nm upon complete protonation of **1a**. The isosbestic point is observed at 520 nm. The pK_a value obtained from Henderson's plot of $\log[(A_0 - A)/(A - A_\infty)]$ *vs* pH is 2.45 for **1a**, where A_0, A_∞, and A are the absorbance of the free base, the fully protonated species, and the mixture of the protonated and the free base forms, respectively. The intercept of the plot on the abscissa corresponds to the pK_a value. The protonated species with a $[Ru_2(\mu\text{-}OH)(\mu\text{-}O_2CR)_2]^{3+}$ core is unstable. The 1-MeIm complex undergoes a facile conversion to the $[Ru_2(\mu\text{-}O)(\mu\text{-}O_2CR)_2]^{3+}$ core whereas the analogous imidazole complex on protonation converts to a monomeric ruthenium(III) species along with the formation of some uncharacterized products. The monomeric complex has been isolated and structurally characterized as $[Ru(ImH)_6](ClO_4)_3$ (**5**).[36,37] This complex has an octahedral geometry giving a Ru(1)−N(1) distance of 2.074(7) Å.

The ^1H NMR spectra of **1**−**3** indicate the essentially diamagnetic nature of the complex. The spectral data are given in Table 4. The methyl protons of the bridging carboxylato ligands appear as a sharp singlet. The aryl protons of the carboxylates are observed as two doublets. The methyl groups of the 1-MeIm ligands show two singlets in the range δ 3.78−4.33 in a 1:2 ratio of peak integration for the ligands trans and cis to the oxide bridge, respectively. Three singlets in a 1:1:1 ratio, observed in the region δ 7.75−8.90, correspond to two protons of the imidazole rings trans to the oxide ligand. The singlets in the region δ 5.65−7.70 are due to the CH protons of the cis-imidazole rings. The peaks are in a 1:1:1 ratio, each corresponding to four protons of the imidazole rings. The ^1H NMR spectral features of **2** and **3** are similar to those of **1** except the NH protons of the imidazole ligands in **2** and **3** which appear as two broad signals in a 1:2 intensity ratio in the range δ 10.4−11.8 and are assignable to the imidazole bases trans and cis to the oxide ligands in **2** and **3**. The significant trans effect of the oxide ligand is observed in the downfield shift of the signals of the trans-imidazole bases compared to those cis to the oxide ligand.

Electrochemistry. The electron transfer behavior of **1**−**3** was studied by cyclic and differential pulse voltammetric techniques using a platinum working electrode in MeCN containing 0.1 M TBAP. The electrochemical data are given in Table 5. Selected voltammograms are shown in Figure 4.

Complex **1** exhibits three voltammetric responses near 0.4, 1.5, and −1.0 V *vs* SCE (Figure 4a). The response at 0.4 V corresponds to a one-electron redox process $Ru^{III}_2/Ru^{III}Ru^{IV}$. The i_{pa}/i_{pc} ratio of unity and the ΔE_p value of 60 mV at v = 20−200 mV s^{-1} indicate the reversibility of the process. The differential pulse voltammogram shows a peak width of 90 mV at half-height indicating the reversible nature of this couple. The response at 1.6 V is due to a quasireversible one-electron oxidation process $Ru^{III}Ru^{IV}/Ru^{IV}_2$, showing a ΔE_p value of 70−

---

(36) Clarke, M. J.; Bailey, V. M.; Doan, P. E.; Hiller, C. D.; LaChance-Galang, K. J.; Daghlian, H.; Mandal, S.; Bastos, C. M.; Lang, D. *Inorg. Chem.* **1996**, *35*, 4896.

(37) Beauchamp, A. L.; Anderson, C. *Inorg. Chem.* **1995**, *34*, 6065.

Table 3. Selected Bond Distances (Å) and Angles (deg) for $[Ru_2O(O_2CMe)_2(ImH)_6](ClO_4)_2\cdot 3H_2O$ (**2a**·$3H_2O$)

molecule A		molecule B	
Ru(1)···Ru(2)	3.272(1)	Ru(3)···Ru(4)	3.273(1)
Ru(1)−O(1)	1.886(3)	Ru(3)−O(6)	1.888(3)
Ru(1)−O(2)	2.119(5)	Ru(3)−O(7)	2.100(4)
Ru(1)−O(4)	2.070(5)	Ru(3)−O(9)	2.081(4)
Ru(1)−N(1)	2.076(6)	Ru(3)−N(13)	2.074(4)
Ru(1)−N(3)	2.128(5)	Ru(3)−N(15)	2.137(6)
Ru(1)−N(5)	2.087(5)	Ru(3)−N(17)	2.064(4)
Ru(2)−O(1)	1.883(2)	Ru(4)−O(6)	1.876(3)
Ru(2)−O(3)	2.053(5)	Ru(4)−O(8)	2.073(3)
Ru(2)−O(5)	2.076(4)	Ru(4)−O(10)	2.082(3)
Ru(2)−N(7)	2.065(6)	Ru(4)−N(19)	2.076(5)
Ru(2)−N(9)	2.119(4)	Ru(4)−N(21)	2.129(4)
Ru(2)−N(11)	2.073(3)	Ru(4)−N(23)	2.083(4)
Ru(1)−O(1)−Ru(2)	120.5(2)	Ru(3)−O(6)−Ru(4)	120.9(2)
N(3)−Ru(1)−N(5)	88.9(2)	N(15)−Ru(3)−N(17)	89.8(2)
N(1)−Ru(1)−N(5)	93.0(2)	N(13)−Ru(3)−N(17)	91.4(2)
N(1)−Ru(1)−N(3)	93.9(2)	N(13)−Ru(3)−N(15)	90.9(2)
O(4)−Ru(1)−N(5)	89.1(2)	O(9)−Ru(3)−N(17)	90.0(2)
O(4)−Ru(1)−N(3)	84.8(2)	O(9)−Ru(3)−N(15)	85.9(2)
O(4)−Ru(1)−N(1)	177.5(2)	O(9)−Ru(3)−N(13)	176.6(2)
O(2)−Ru(1)−N(5)	173.7(2)	O(7)−Ru(3)−N(17)	175.4(2)
O(2)−Ru(1)−N(3)	85.9(2)	O(7)−Ru(3)−N(15)	85.6(2)
O(2)−Ru(1)−N(1)	83.8(2)	O(7)−Ru(3)−N(13)	88.0(2)
O(2)−Ru(1)−O(4)	94.0(2)	O(7)−Ru(3)−O(9)	90.3(2)
O(1)−Ru(1)−N(5)	89.1(2)	O(6)−Ru(3)−N(17)	88.7(2)
O(1)−Ru(1)−N(3)	175.6(2)	O(6)−Ru(3)−N(15)	178.1(2)
O(1)−Ru(1)−N(1)	90.1(2)	O(6)−Ru(3)−N(13)	90.2(2)
O(1)−Ru(1)−O(4)	91.3(2)	O(6)−Ru(3)−O(9)	93.0(2)
O(1)−Ru(1)−O(2)	96.3(2)	O(6)−Ru(3)−O(7)	95.9(2)
N(9)−Ru(2)−N(11)	90.7(2)	N(21)−Ru(4)−N(23)	93.0(2)
N(7)−Ru(2)−N(11)	90.4(2)	N(19)−Ru(4)−N(23)	93.3(2)
N(7)−Ru(2)−N(9)	88.3(2)	N(19)−Ru(4)−N(21)	91.3(2)
O(5)−Ru(2)−N(11)	175.1(2)	O(10)−Ru(4)−N(23)	176.3(2)
O(5)−Ru(2)−N(9)	84.6(2)	O(10)−Ru(4)−N(21)	83.2(2)
O(5)−Ru(2)−N(7)	88.3(2)	O(10)−Ru(4)−N(19)	86.9(2)
O(3)−Ru(2)−N(11)	88.8(2)	O(8)−Ru(4)−N(23)	88.8(2)
O(3)−Ru(2)−N(9)	89.2(2)	O(8)−Ru(4)−N(21)	86.6(2)
O(3)−Ru(2)−N(7)	177.3(2)	O(8)−Ru(4)−N(19)	177.1(2)
O(3)−Ru(2)−O(5)	92.3(2)	O(8)−Ru(4)−O(10)	90.9(2)
O(1)−Ru(2)−N(11)	88.3(2)	O(6)−Ru(4)−N(23)	88.3(2)
O(1)−Ru(2)−N(9)	179.0(2)	O(6)−Ru(4)−N(21)	178.3(2)
O(1)−Ru(2)−N(7)	91.9(2)	O(6)−Ru(4)−N(19)	89.7(2)
O(1)−Ru(2)−O(5)	96.4(2)	O(6)−Ru(4)−O(10)	95.4(2)
O(1)−Ru(2)−O(3)	90.6(2)	O(6)−Ru(4)−O(8)	92.4(2)

80 mV and a i_{pa}/i_{pc} ratio of unity at various scan rates. The voltammogram observed near −1.0 V corresponds to a one-step two-electron reduction process Ru^{III}_2/Ru^{II}_2. The two-electron stoichiometry of this redox process is obtained from the controlled-potential coulometric measurements at a cathodic potential of −1.3 V giving an n value of 2.09. The i_{pc}/i_{pa} ratio of unity and a ΔE_p value of 30−50 mV at v = 20−100 mV s^{-1} suggest the quasireversible nature of the couple. The couples involved are given in eq 2, where **1′** denotes the $\{Ru_2(\mu\text{-}O)(\mu\text{-}O_2CR)_2\}^{2+}$ core of **1**.

$$\underset{\mathbf{1'}^{2+}}{\{Ru^{IV}_2(\mu\text{-}O)(\mu\text{-}O_2CR)_2\}^{4+}} \underset{-e^-}{\overset{+e^-}{\rightleftharpoons}} \underset{\mathbf{1'}^{+}}{\{Ru^{III}Ru^{IV}(\mu\text{-}O)(\mu\text{-}O_2CR)_2\}^{3+}} \underset{-e^-}{\overset{+e^-}{\rightleftharpoons}} \underset{\mathbf{1'}}{\{Ru^{III}_2(\mu\text{-}O)(\mu\text{-}O_2CR)_2\}^{2+}} \underset{-2e^-}{\overset{+2e^-}{\rightleftharpoons}} \underset{\mathbf{1'}^{2-}}{\{Ru^{II}_2(\mu\text{-}O)(\mu\text{-}O_2CR)_2\}} \tag{2}$$

Complexes **2** and **3** show two one-electron oxidation processes near 0.4 and 1.6 V *vs* SCE (Figure 4b). While the oxidation process $Ru^{III}_2/Ru^{III}Ru^{IV}$ with a ΔE_p value of 60 mV is reversible, the $Ru^{III}Ru^{IV}/Ru^{IV}_2$ couple showing a ΔE_p value of 70−80 mV at various scan rates and an i_{pa}/i_{pc} ratio of unity is quasireversible. The 1-methylimidazole ligand is redox inactive in the potential limit +1.8 to −1.9 V *vs* SCE. The imidazole and 4-methylimidazole bases exhibit a quasireversible cyclic voltammetric response at −1.4 V (ΔE_p = 200 mV at 50 mV s^{-1}) in MeCN−0.1 M TBAP. However, complexes **2** and **3** are redox inactive in the negative potential limit up to −1.9 V *vs* SCE. It is interesting to note that the $Ru^{III}_2/Ru^{III}Ru^{IV}$ couple in **1**−**3** shows an excellent Nernstian behavior even though the Ru−Ru and Ru−O$_{oxo}$ distances and the Ru−O$_{oxo}$−Ru angle among the $[Ru_2(\mu\text{-}O)]^{n+}$ (n = 4, 5) units are significantly different from each other as observed in the crystal structures of **1a** and **4a**·$1.5H_2O$.

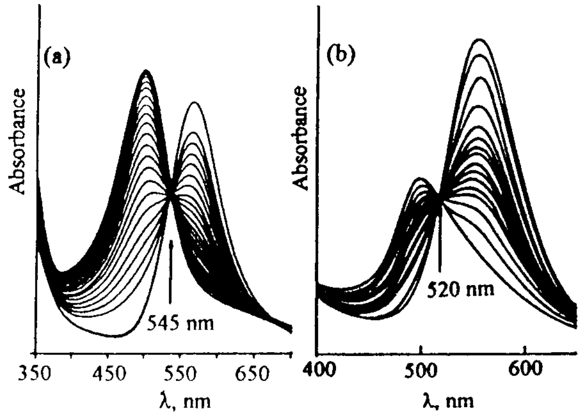

Figure 3. (A) Visible absorption spectra at 25 °C showing the progress of the reaction between $[Ru_2O(O_2CMe)_2(1\text{-}MeIm)_6](ClO_4)_2$ (**1a**) in MeCN and $K_2S_2O_8$ in water. (B) Visible spectral record of protonation of **1a** in MeCN with $HClO_4$ at 25 °C.

Multielectron transfer reactions in transition metal complexes are of considerable interests from chemical as well as biological point of view.[2,38] Polynuclear complexes, especially the trinuclear complexes of ruthenium, act as versatile electrocatalysts involving multielectron redox processes occurring over a wide potential range.[39] Various mononuclear complexes also show metal-centered multielectron transfer redox processes.[40] In binuclear systems a general observation is that when there is insignificant interactions between the metal centers, simultaneous oxidation of the metal ions could take place at the same potential leading to a single-step two-electron transfer process.[14,41] But in strongly coupled dimeric complexes, simultaneous oxidation or reduction of the metal centers is energetically difficult, as one metal ion, while undergoing electronic change, affects the other metal center. In some complexes, an irreversible two-electron transfer process is known to take place and an ECE mechanism[13] is involved in the conversion of the product.

A comparison of the electrochemical data on the complexes with a $[Ru_2(\mu\text{-}O)(\mu\text{-}O_2CR)_2]^{2+}$ core reveals that only a few complexes show two consecutive one-electron reductions along with the oxidation processes.[17,20,21] The reversibility of the first

---

(38) Kramarz, K. W.; Norton, J. R. *Prog. Inorg. Chem.* **1994**, *42*, 1.

(39) Abe, M.; Sasaki, Y.; Yamada, Y.; Tsukhara, K.; Yano, S.; Ito, T. *Inorg. Chem.* **1995**, *35*, 4490.

(40) Chan, C.-W.; Lai, T.-F.; Che, C.-M. *J. Chem. Soc., Dalton Trans.* **1994**, 895. Wang, Y.-P.; Che, C.-M.; Wong, K.-Y.; Peng, S.-M. *Inorg. Chem.* **1993**, *32*, 5827. Diamantis, A.-A.; Murphy, W. R., Jr.; Meyer, T. J. *Inorg. Chem.* **1984**, *23*, 3230. Ram, M. S.; Johnson, C. S.; Blackbourn, R. L.; Hupp, J. T. *Inorg. Chem.* **1990**, *29*, 238. Mohanty, J. G.; Chakravorty, A. *Inorg. Chem.* **1976**, *15*, 2912.

Table 4. ^{1}H NMR Spectral Data[a] for the Complexes $[Ru_2O(O_2CR)_2(1\text{-MeIm})_6](ClO_4)_2$ (**1**), $[Ru_2O(O_2CR)_2(ImH)_6](ClO_4)_2$ (**2**), and $[Ru_2O(O_2CR)_2(4\text{-MeImH})_6](ClO_4)_2$ (**3**) (R = Me, (**a**), C_6H_4-*p*-X (X = OMe (**b**), Me (**c**))

	δ/ppm and multiplicity (J/Hz)							
		imidazole base						
complex	$Me(O_2CR)^b$	Me trans^b	Me cis^c	CH trans^d	CH cis^e	NH trans^d	NH cis^e	aryl H $(O_2CR)^e$
1a	1.49 s	4.29 s	3.80 s	7.78 s	5.67 s			
				7.91 s	6.62 s			
				8.61 s	7.58 s			
1b	3.71 s	4.33 s	3.79 s	7.80 s	5.80 s			6.61 d (9)
				8.17 s	6.56 s			7.23 d (8)
				8.80 s	7.26 s			
1c	2.24 s	4.33 s	3.78 s	7.82 s	5.77 s			6.91 d (8)
				8.20 s	6.56 s			7.17 d (8)
				8.87 s	7.66 s			
2a	1.42 s			7.83 s	6.31 s	11.64 s	10.49 s	
				8.07 s	6.82 s			
				8.60 s	6.97 s			
2b	3.68 s			7.98 s	6.42 s	11.71 s	10.60 s	6.63 d (9)
				8.13 s	6.93 s			7.21 d (9)
				8.73 s	7.18 s			
3a	1.40 s	2.66 s	2.09 s	7.51 s	5.98 s	11.57 s	10.54 s	
				8.38 s	6.64 s			
3b	3.69 s	2.71 s	2.02 s	7.65 s	6.15 s	11.69 s	10.61 s	7.21 d (9)
				8.53 s	6.76 s			6.65 d (9)

[a] $CDCl_3$ for **1**. CD_3CN for **2** and **3**. [b] No. of H = 6. [c] No. of H = 12. [d] No. of H = 2. [e] No. of H = 4.

Table 5. Cyclic and Differential Pulse Voltammetric Data[a] for $[Ru_2O(O_2CR)_2(1\text{-MeIm})_6](ClO_4)_2$ (**1**), $[Ru_2O(O_2CR)_2(ImH)_6](ClO_4)_2$ (**2**), and $[Ru_2O(O_2CR)_2(4\text{-MeImH})_6](ClO_4)_2$ (**3**) in MeCN−0.1 M TBAP (R = Me (**a**), C_6H_4-*p*-X (X = OMe (**b**), Me (**c**))

	$Ru^{III}Ru^{IV} \rightleftharpoons Ru^{IV}_2$		$Ru^{III}_2 \rightleftharpoons Ru^{III}Ru^{IV}$		$Ru^{III}_2 \rightleftharpoons Ru^{II}_2$	
complex	$E_{1/2}$ (ΔE_p)	E_{CO} (δ)	$E_{1/2}$ (ΔE_p)	E_{CO} (δ)	$E_{1/2}$(ΔE_p)	E_{CO} (δ)
1a	1.52 (80)	1.51 (100)	0.36 (60)	0.35 (95)	−1.07 (30)	−1.10 (60)
1b	1.55 (90)	1.54 (100)	0.39 (60)	0.38 (90)	-0.98 (30)	-0.97 (65)
1c	1.57 (60)	1.54 (100)	0.39 (60)	0.41 (90)	-0.98 (40)	−1.00 (80)
2a	1.57 (60)	1.57 (100)	0.35 (60)	0.36 (90)		
2b	1.57 (60)	1.58 (100)	0.41 (60)	0.40 (90)		
3a	1.56 (80)	1.55 (100)	0.37 (60)	0.37 (95)		
3b	1.55 (90)	1.54 (100)	0.37 (60)	0.37 (95)		

[a] CV data: $E_{1/2} = (E_{pa} + E_{pc})/2$ in V; $\Delta E_p = E_{pa} - E_{pc}$ in mV; $v = 20$ mV s^{-1}. DPV data: E_{CO}, crossover potential in V; δ, peak width at half-height in mV; $v = 5$ mV s^{-1}; modulation amplitude = 25 mV (p−p); drop time = 0.5 s. All potentials are versus SCE at 298 K.

reduction process is always better than the second. In some cases only one reduction process has been observed.[18,22] Other metal complexes with a $[M_2(\mu\text{-O})(\mu\text{-}O_2CR)_2]^{2+}$ core (M = Fe, Mn, Mo, V, etc.) show, in general, a single irreversible one-electron reduction process.[11,14,42] Complex **1** is the first species with a (μ-oxo)bis(μ-carboxylato)dimetal core showing a quasi-reversible one-step two-electron transfer reduction process.[7,9b,16,20,26]

The electrochemical behavior of **1**−**3** has similarity to the redox properties of a structurally analogous mixed-ligand species $[Ru_2(\mu\text{-O})(\mu\text{-}O_2CMe)_2(bpy)_2L_2](ClO_4)_2$, exhibiting a one-electron oxidation and two consecutive one-electron reduction processes (L, 1-MeIm, ImH, 4-MeImH).[23,24] While the Ru^{III}_2/$Ru^{III}Ru^{IV}$ and Ru^{III}_2/Ru_2(III,II) processes are nearly reversible, the Ru_2(III,II)/Ru^{II}_2 process is irreversible. Like in **1**−**3**, the HOMO level in these complexes, which is involved in the oxidation process at 0.77 V *vs* SCE, is not sensitive to the nature of the substituent on the imidazole base. The LUMO level, however, varies depending on the imidazole base. The reduction couples for the 1-MeIm complex at potentials −0.57 and −0.90 V *vs* SCE are considerably different from the values of −0.85 and −1.56 V observed for the ImH and 4-MeImH complexes. In presence of a weak proton donor base the complexes show a one-step two-electron transfer process at −0.40 V for the 1-MeIm and at −0.60 V for the ImH and 4-MeImH complexes. The difference of 200 mV is significant considering the presence of only one terminal imidazole base on each metal center. The difference between the LUMO levels of $[Ru_2(\mu\text{-O})(\mu\text{-}O_2CMe)_2(bpy)_2(1\text{-MeIm})_2]^{2+}$ and $[Ru_2(\mu\text{-O})(\mu\text{-}O_2CMe)_2(1\text{-MeIm})_6]^{2+}$, showing the two-electron transfer reduction process, is 600 mV. It is possible that the energy of the LUMO level in **2** and **3** is much higher and is beyond the observed solvent cut-off limit of −1.9 V.

The plausible explanation for the two-electron transfer process in **1** is the protonation of the oxide bridge under reduced condition leading to the merger of two one-electron reduction processes. The diruthenium(II) core is expected to be basic enough to remove proton from the water present in MeCN as

---

(41) Strouse, G. F.; Schoonover, J. R.; Duesing, R.; Boyde, S.; Jones, W. E., Jr.; Meyer, T. J. *Inorg. Chem.* **1995**, *34*, 473. Bardwell, D. A.; Barigelletti, F.; Cleary, R. L.; Flamigni, L.; Guardigli, M.; Jeffery, J. C.; Ward, M. D. *Inorg. Chem.* **1995**, *34*, 2438. Wang, P.-W.; Fox, A. M. *Inorg. Chem.* **1995**, *34*, 36. Baba, A. I.; Ensley, H. E.; Schmehl, R. H. *Inorg. Chem.* **1995**, *34*, 1198. Geilenkirchen, A.; Neubold, P.; Schneider, R.; Wieghardt, K.; Florke, U.; Haupt, H.-J.; Nuber, B. *J. Chem. Soc., Dalton Trans.* **1994**, 457. Haga, M.; Ali, M. M.; Maegawa, H.; Nozaki, K.; Yoshimura, A.; Ohno, T. *Coord. Chem. Rev.* **1994**, *132*, 99. Kelson, E. P.; Henling, L. M.; Schaefer, W. P.; Labinger, J. A.; Bercaw, J. E. *Inorg. Chem.* **1993**, *32*, 2863. Vogtle, F.; Frank, M.; Nieger, M.; Belser, P.; von Zelewsky, A.; Balzani, V.; Barigelletti, F.; de Cola, L.; Flamigni, L. *Angew. Chem., Int. Ed. Engl.* **1993**, *32*, 1643. Belser, P.; von Zelewsky, A.; Frank, M.; Steel, C.; Vogtle, F.; De Cola, L.; Barigelletti, F.; Balzani, V. *J. Am. Chem. Soc.* **1993**, *15*, 4076.

(42) Beer, R. H.; Tolman, W. B.; Bott, S. G.; Lippard, S. J. *Inorg. Chem.* **1991**, *30*, 2082.

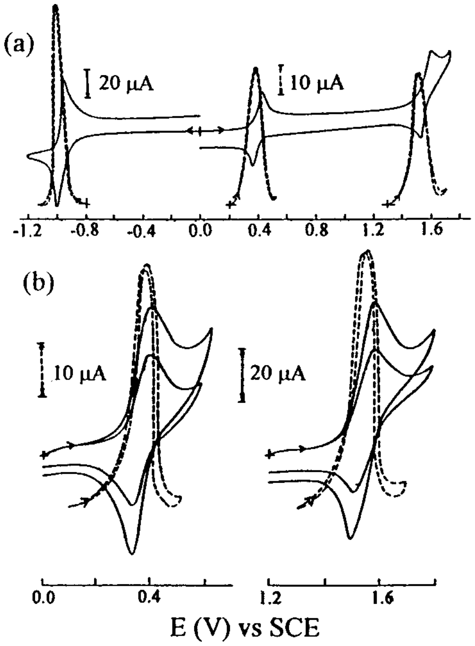

Figure 4. (a) Cyclic (—) and differential pulse (- - -) voltammograms of $[Ru_2O(O_2CC_6H_4\text{-}p\text{-}Me)_2(1\text{-}MeIm)_6](ClO_4)_2$ (**1c**) in MeCN−0.1 M TBAP at scan rates 50 mV s^{-1} (CV) and 2 mV s^{-1} (DPV). (b) Cyclic and differential pulse voltammograms of $[Ru_2O(O_2CC_6H_4\text{-}p\text{-}OMe)_2(4\text{-}MeImH)_6](ClO_4)_2$ (**3b**) in MeCN−0.1 M TBAP at scan rates 50 mV s^{-1} (CV) and 2 mV s^{-1} (DPV).

an impurity to protonate the oxide bridge. In presence of a proton-donor base like *p*-toluenesulfonic acid, the two-electron response splits into two one electron waves.[24] What is interesting in the present investigation is the quasireversiblity of the two-electron transfer process. One possibility is that the presence of imidazole bases renders flexibility to the core structure toward addition or removal of electrons from the $[Ru_2O(O_2CR)_2]^{2+}$ core.

Conclusion

Diruthenium complexes having a (μ-oxo)bis(μ-carboxylato)diruthenium(III) core with six unidentate imidazole bases as terminal ligands have been prepared by a novel core conversion reaction using $Ru_2Cl(O_2CR)_4$ as a precursor. Two diruthenium(III) complexes containing imidazole and 1-methylimidazole ligands and a diruthenium(III,IV) complex having 1-methylimidazole ligand have been structurally characterized. The essentially diamagnetic diruthenium(III) complexes retain their tribridged core structure in solution as evidenced from the ^1H NMR spectral studies. The complexes are redox active. Complex **1** exhibits two one-electron oxidation $Ru^{III}_2/Ru^{III}Ru^{IV}$ and $Ru^{III}Ru^{IV}/Ru^{IV}_2$ and one two-electron reduction Ru^{III}_2/Ru^{II}_2 couples. Complexes **2** and **3** display only two oxidation processes, and no reduction of the core has been observed. Interestingly, the $Ru^{III}_2/Ru^{III}Ru^{IV}$ couple is reversible although the core structural parameters of the diruthenium(III) and diruthenium(III,IV) units differ considerably from each other. The one-step two-electron transfer process Ru^{III}_2/Ru^{II}_2 is quasi-reversible. Observation of such an electron-transfer process is significant considering its relevance to the electron-transfer behavior of the respiratory protein hemerythrin (Hr) cycling between the diferrous deoxyHr and the diferric oxyHr forms involving a rapid and reversible proton-coupled two-electron transfer process resulting from the binding of a dioxygen molecule to one deoxyHr iron site.

Acknowledgment. We are grateful to Prof. A. Chakravorty of the Indian Association for the Cultivation of Science, Calcutta, India, for the coulometric data. This work is supported by the Department of Science and Technology, Government of India. We thank the Alexander von Humboldt Foundation in Germany for a donation of an electroanalytical system.

Supporting Information Available: An ^1H NMR spectrum of $[Ru_2O(O_2CC_6H_4\text{-}p\text{-}OMe)_2(ImH)_6](ClO_4)_2$ and an ORTEP diagram of the cationic complex in $[Ru(ImH)_6](ClO_4)_3$ (2 pages). X-ray crystallographic files, in CIF format, are available on the Internet only. Ordering and access information is given on any current masthead page.

IC970390Z